[3] Ukanwa, A. O., Stermole, F. J., and Golden, J. O., "Phase Change Solidification Dynamics," *Journal of Spacecraft and Rockets*, Vol. 8, No. 2, Feb. 1971, pp. 193–196.

[4] Shah, A. P., "A Microscopic and Thermal Study of the Solidification of n-octadecane," Thesis T-1334, 1970, Colorado School of Mines, Golden, Colo.

[5] Bentilla, E. W., Stewart, K. F., and Kane, L. E., Final Rept., Contract NAS8-11163, April 1966, Northrup Space Laboratories, Hawthorne, Calif.

[6] Bain, R. L., "The Effect of Gravity-Induced Free Convection Upon the Melting Phenomena of a Finite Paraffin Slab," Thesis T-1319, 1970, Colorado School of Mines, Golden, Colo.

[7] Carslaw, H. S. and Jaeger, J. C., *Conduction of Heat in Solids*, Oxford University Press, London, 1959, pp. 281–296.

Heat-Transfer Correlations for Blunt Cones at Angle of Attack

GEORGE F. WIDHOPF*
The Aerospace Corporation, San Bernardino, Calif.

THE prediction of heat-transfer rates over a blunt cone at angle of attack is a complex numerical problem at best. In any comprehensive analysis, the influence of three-dimensional effects, as well as entropy swallowing, must be included. The inclusion of either of these effects is not a trivial task. Thus, it would be useful to have an effective means of computing the surface heat transfer without the necessity of determining the detailed flow environment for every individual case. This Note presents a convenient correlation of the local heat-transfer rate with the local surface pressure for blunt cones at angles of attack. The correlation is demonstrated utilizing two sets of experimental data; one for the turbulent case and one for the laminar case.

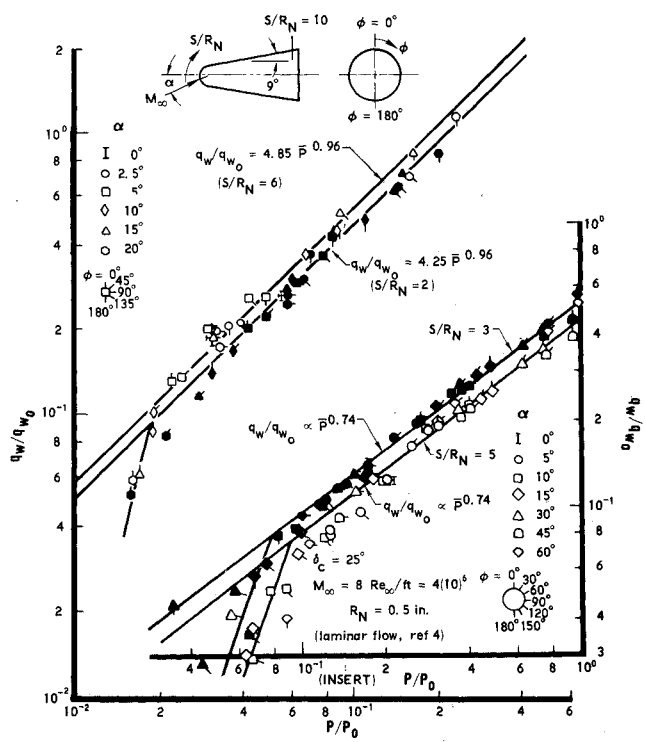

Fig. 1 Correlation of turbulent data at stations S/R_N = 2 and 6. Insert: Correlation of laminar data from Ref. 4.

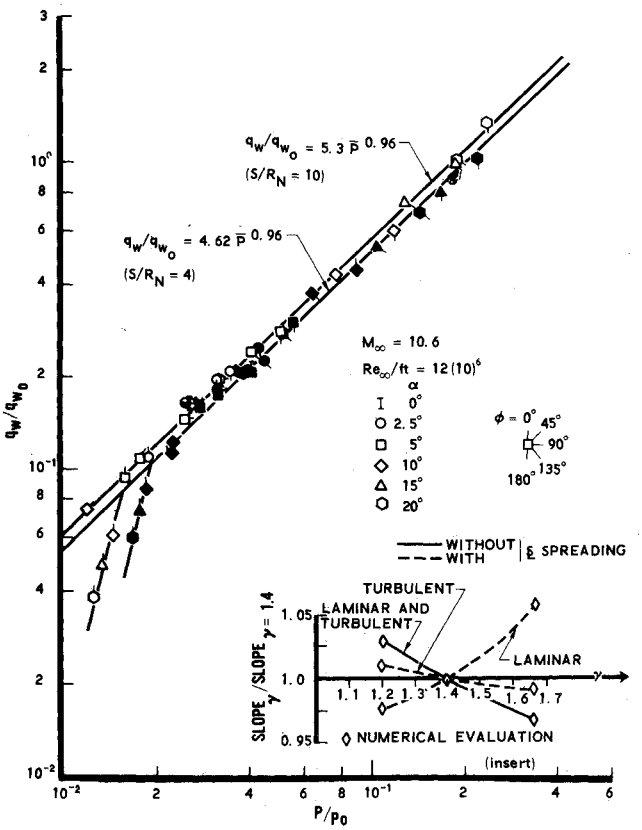

Fig. 2 Correlation of turbulent data at stations S/R_N = 4 and 10. Insert: Variation of slope with γ.

Detailed distributions of the turbulent heat-transfer rate and surface pressure measured on a blunt (R_N = 2.5 in.), 9°, half-angle cone at angles of attack of α = 0°, 2.5°, 5°, 10°, 15° and 20° were presented in Ref. 1. The measurements were made in a nitrogen environment at M_∞ = 10.6 and Re_∞/ft = 12(10)^6. There, the similarity between the heat transfer and surface pressure contours was noticed. Further analysis of the pressure and heat-transfer data was performed to determine the extent and nature of the similarity. The results, plotted in logarithmic coordinates, are shown in Figs. 1 and 2 for various locations on the conical surface measured in the angle-of-attack coordinate system depicted. Here, the local values of the turbulent heat-transfer rate nondimensionalized with respect to the measured laminar stagnation rate (q_w/q_{w_0}) are plotted against the corresponding value of the surface pressure nondimensionalized with respect to the stagnation point pressure ($p/p_0 = \bar{p}$). At each station, data corresponding to the indicated circumferential locations were plotted for each angle of attack discussed previously.

These results show that at each specific S/R_N station, the data can be correlated (within ±12%, or approximately the accuracy of the data itself) by a straight line of slope 0.96. Thus, at each station, data for various circumferential locations corresponding to various angles of attack can all be correlated by a line of a single slope over a one and one-half order of magnitude variation in pressure and heat transfer. It is also interesting to note that the data in the separated region seems to also follow a definite trend.

In Ref. 1, it was shown that the turbulent heat transfer formulation proposed by Vaglio-Laurin[2] is a good approximation in a three-dimensional environment. In those calculations, inviscid surface streamlines were traced over the cone utilizing the experimental pressure distribution, and the heat-transfer rate calculated along each streamline. Thus, the effect of streamline spreading was included in the prediction

Received April 16, 1971. The author would like to thank F. Fernandez for some helpful suggestions and comments.

* Member of the Technical Staff. Associate Member AIAA.

of the heat-transfer rate, but entropy swallowing was neglected. For the zero angle-of-attack case, it was shown that the inclusion of the effect of entropy swallowing improved the computation, thereby indicating that this formulation was probably a good approximation over most of the surface providing the local conditions are evaluated properly.

The results obtained utilizing the analysis described in Ref. 1 were analyzed, and it was found that at each station they could also be correlated (±7%) in the manner described above, although the evaluated slope was different than the one determined from the experimental data. When the effect of streamline spreading on the local heat-transfer rate was either included or neglected, the slope was evaluated to be 0.77 and 0.70, respectively (see Fig. 3). It should be noticed that the neglection of entropy swallowing is a good approximation over a significant range of conditions. In view of these experimental and numerical results, it is expected that when the effect of entropy swallowing is included the numerical results should still exhibit the same correlation behavior, except that the slope of the resultant power law should more closely approximate the one derived from the experimental data.

At each station, the absolute level of the power law correlation curve was found to be predicted very accurately (±3%) by the $\alpha = 0°$ results, when they were calculated including the effect of entropy swallowing.

Some additional information regarding the dependence of q_w/q_{w_0} on $\bar{p}$ can be obtained by examining the analytic expressions for the local heat-transfer rate. Assuming a perfect gas and neglecting entropy swallowing, the following expression can be derived under hypersonic conditions utilizing Vaglio-Laurin's turbulent heat-transfer formulation[2] and the Fay and Riddell[3] relationship for the laminar stagnation heat-transfer rate

$$q_w/q_{w_0} = C(T_w/T_\infty)^{[(1-w)/10]}(Re_\infty R_N)^{3/10}M_\infty^{-(2w+1)/5}\cdot \bar{p}^{[w(\gamma-1)+1]/\gamma}(1-\bar{p})^{(\gamma-1)/2\gamma}\bar{h}_2^{1/4}\cdot \left\{\int_0^{\bar{l}} \bar{p}^{[w\gamma+(1-w)]/\gamma}(1-\bar{p})^{(\gamma-1)/2\gamma}\bar{h}_2^{5/4}\,d\bar{l}\right\}^{-1/5} \quad (1)$$

where h_2 is a length element which characterizes the spreading of the inviscid streamlines and is given by the following relationship[2]

$$\bar{h}_2 = h_2/R_N = \frac{(\gamma-1)}{2\gamma\bar{K}_n\tan\eta}\,\bar{p}^{-1/\gamma}(1-\bar{p})^{(1-\gamma)/\gamma}\frac{\partial\bar{p}}{\partial\bar{x}_2} \quad (2)$$

Here C is a function of ratio of the specific heats (γ) and the Prandtl number; M_∞, Re_∞, and T_∞ are the freestream Mach number, Reynolds number per unit length, and temperature, respectively; T_w is the wall temperature; $\bar{K}_n$ and η are geometric parameters defined in Ref. 2 and $\bar{x}_2$ is the surface coordinate normal to the streamline direction $\bar{l}$, both of which are nondimensionalized with respect to the nose radius. The relation $\mu \propto T^w$ has been utilized in this derivation for the sake of simplicity.

The Re_∞ dependence shown in Eq. (1) was checked utilizing additional data obtained during the test program described in Ref. 1. Here the heat-transfer ratio at a given location was plotted as a function of Re_∞. This was done for various surface locations at each angle of attack considered. In each case, the variation of the heat-transfer ratio with Re_∞ was found to be prescribed very well by a 0.3 power law, thereby validating this dependence as well as the extension of the correlation for these experimental conditions over the Re_∞ range including 8–12(10)^6/1 ft. (See Ref. 6.)

Equation (1) also indicates that, to this approximation, the dependence of q_w/q_{w_0} on $\bar{p}$ is a function only of the gas properties γ and w. Calculations analogous to those described previously were made for different γ's (using calculated pressure distributions) in order to determine, under these approximations, the variation of the correlation slope with

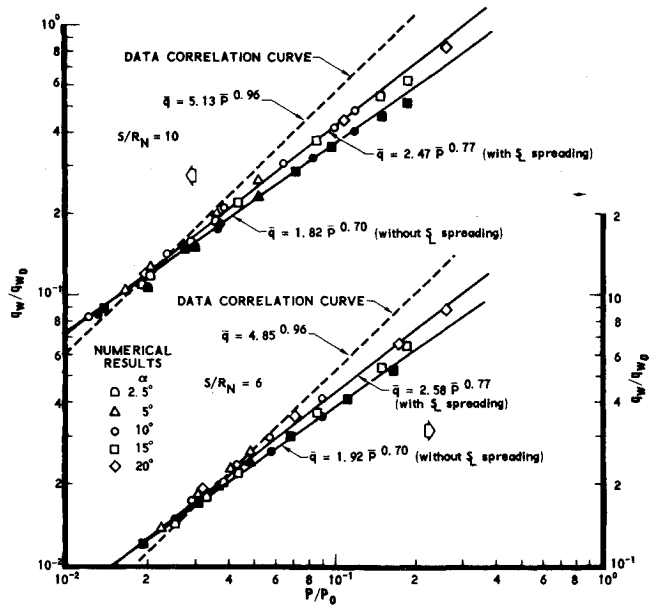

Fig. 3 Correlation of numerical results for turbulent case at stations $S/R_N = 10$ and 6.

γ. In these calculations, the viscosity was evaluated utilizing a Sutherland formula with constant coefficients. The results are shown in the insert of Fig. 2. Here it is seen that the variation of the slope is very weak when streamline spreading is neglected and is effectively independent of γ when streamline spreading is included. Further experimental data are needed to determine or affirm the actual dependence and variation of the slope.

The same procedure was utilized to investigate the laminar flow case. Measurements of the laminar heat-transfer rate and static pressure distributions on a blunt ($R_N = 0.5$ in.), 25°, half-angle cone at angles of attack of $\alpha = 0°$, 5°, 10°, 15°, 30°, 45° and 60° were reported in Ref. 4.† The tests were conducted in an air environment at $M_\infty = 8$ and Re_∞/ft of 4(10)^6 and 0.89(10)^6. Typical results are shown in the insert of Fig. 1.

As in the turbulent case, the data can be correlated (within ±15%) at each station‡ by a set of power laws, each having a slope of 0.74. Again, the absolute levels of the correlation curves are predicted by the $\alpha = 0°$ distribution, when it is calculated including the effect of entropy swallowing. Numerical calculations analogous to those made for the turbulent case could also be correlated in this manner yielding slopes of 0.68 when the effect of streamline spreading is included and 0.5 when it is neglected.

Utilizing Vaglio-Laurin's laminar heat-transfer formulation[5] and proceeding in the same manner as was used in deriving Eq. (1), the following result is obtained

$$\frac{q_w}{q_{w_0}} = C_1\bar{p}^{[\gamma+4+4w(\gamma-1)]/5\gamma}(1-\bar{p})^{(\gamma-1)/2\gamma}\bar{h}_2\cdot \left\{\int_0^{\bar{l}} \bar{p}^{[\gamma+4+4w(\gamma-1)]/5\gamma}(1-\bar{p})^{(\gamma-1)/2\gamma}\bar{h}_2^2\,d\bar{l}\right\}^{-1/2} \quad (3)$$

which is independent of R_N and Re_∞ (except in regions where viscous-inviscid interactions are important and $\bar{p}$ becomes Re_∞ dependent). The Re_∞ independence was substantiated by the sets of data presented in Ref. 4. (See Ref. 6.) Again, the dependence of q_w/q_{w_0} on $\bar{p}$ is only a function of γ and w. The variation of the correlation slope with γ was evaluated

† Tabulations of these data were supplied by I. Beckwith of NASA-Langley.

‡ A more comprehensive set of figures for both the laminar and turbulent cases is contained in Ref. 6.

in the same manner as was used for the turbulent case. The results are analogous to those obtained in the turbulent case and are shown in the insert of Fig. 2.

Thus, a calculation of the zero angle-of-attack distribution together with a detailed surface pressure distribution should allow for a quick evaluation of the turbulent or laminar heat-transfer distribution at various circumferential locations over a blunt cone at various angles of attack. This has been demonstrated for two sets of data. The extension of this type of correlation to conditions other than that described herein has been indicated, but this must be verified experimentally.

References

[1] Widhopf, G. F., "Turbulent Heat Transfer Measurements on a Blunt Cone at Angle of Attack," TR-0059(S6816-66)-1, Feb. 1971, The Aerospace Corp., San Bernardino, Calif.

[2] Vaglio-Laurin, R., "Turbulent Heat Transfer on Blunt-Nosed Bodies in Two-Dimensional and General Three-Dimensional Hypersonic Flow," *Journal of the Aerospace Sciences*, Vol. 27, No. 1, Jan. 1960, pp. 27–36.

[3] Fay, J. A. and Riddell, F. R., "Theory of Stagnation Point Heat Transfer in Dissociated Air," *Journal of the Aeronautical Sciences*, Vol. 25, No. 2, Feb. 1958, pp. 73–85.

[4] Bushnell, D. M., Jones, R. A., and Huffman, J. K., "Heat Transfer and Pressure Distributions on Spherically Blunted 25° Half Angle Cone at Mach 8 and Angles of Attack up to 90°," TN-D-4792, Oct. 1968, NASA.

[5] Vaglio-Laurin, R., "Laminar Heat Transfer on Three-Dimensional Blunt Nosed Bodies in Hypersonic Flow," *American Rocket Society Journal*, Vol. 29, No. 2, Feb. 1959, pp. 123–129.

[6] Widhopf, G. F., "Heat Transfer Correlations for Blunt Cones at Angle of Attack," TR-0172(S2816-63)-1, July 1971, The Aerospace Corp., San Bernardino, Calif.

Measurements of Shock Wave Location in Hypersonic Nitrogen Flow

MERVIN E. HILLARD JR.,* WILLIAM D. HARVEY,† AND M. LAWRENCE EMORY‡

NASA Langley Research Center, Hampton, Va.

WHEN a high-energy electron beam interacts with a flowing gas, two sources of radiation may be used to visualize the flow structure: the fluorescence from direct excitation[1,2] and afterglow[3,4]; both sources have been used in flowing nitrogen gas media to study plumes and flow fields about simple configurations. This Note describes the technique of electron-beam flow visualization used in the Mach 19 Hypersonic Nitrogen Facility[5] for quantitative studies of complex, three-dimensional shock waves about a space-shuttle configuration.

The electron gun and drift tube assembly[6] were mounted on top of the tunnel at the centerline (Fig. 1a), and static and dynamic calibrations of the beam deflection circuit were made. Two 35 mm cameras positioned at the side and on top of the tunnel recorded the flow patterns at a tunnel stagnation pressure and temperature of 2.4×10^7 N/m^2 and 1.65×10^3 °K.

Received March 25, 1971; revision received July 6, 1971.

Index categories: Entry Vehicles and Landers; Supersonic and Hypersonic Flow.

* Aero-Space Technologist, Instrument Research Division, Gas Parameters Measurements Section.

† Aero-Space Technologist, Hypersonic Vehicles Division, Gas Dynamics Section. Member AIAA.

‡ Engineering Technician, Instrument Research Division, Gas Parameters Measurements Section.

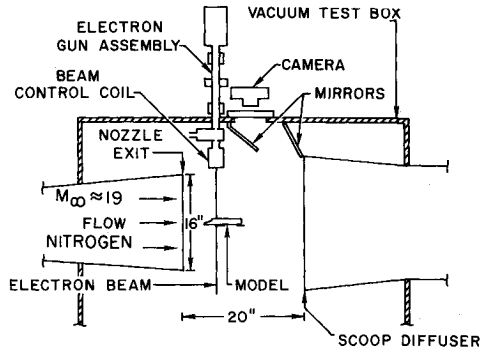

A) EXPERIMENTAL SETUP

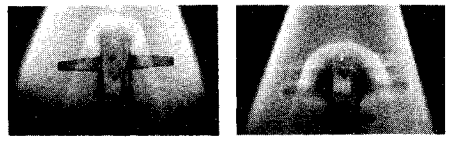

B) METHOD 1, α = 0°

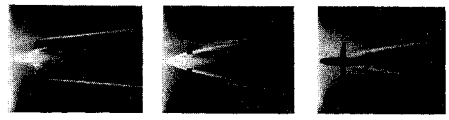

C) METHOD 2. α = 15°

Fig. 1 Experimental setup and typical sequences of two-dimensional cross sections through the shock structure.

Two methods were used to visualize the flow. First, the beam was swept in a plane perpendicular to the flow, and the position of this plane in the flow direction was varied in discrete steps; photographs, looking upstream at the model, were taken at each position of the beam plane (Fig. 1b). In this method the directly excited fluorescence produced in the plane of the beam enhanced the shock structure. Second, a collimated beam was stepped across the flow upstream of the model, and through the side window a photograph was taken at each step of the beam to show two-dimensional "slices" of the flow structure (Fig. 1c). The beam position calibration determined the location of each slice with respect to the model and the afterglow enhanced the flowfield.

In the initial quantitative tests, the flowfield about a sharp flat plate (0.13 m wide and 0.20 m long) at zero angle of attack was studied. The second method was used to map the flow structure about the flat plate, and for the data in this note, the beam was positioned to illuminate a slice through the shock layer along the center of the plate. Parameters calculated from measurements of the photographs included shock wave location (outer edge) y_s, boundary-layer thickness y_δ, and density ratio across the shock ρ_{max}/ρ_∞. (The effect on the data of varying film exposure was not investigated.) Figure 2a shows the shock wave location determined from the flow visualization photographs and, for comparison, two empirical calculations[7,8] and measurements of the shock location based on pitot pressure (P_{t_2}) data and schlieren photographs. (Details on construction and dimensions of pressure and temperature probes are available in Ref. 9.) The shock position from the pitot probe measurements was chosen as the location of the maximum in pressure (see insert, Fig. 2a). The flow visualization photographs also showed a bright region extending from the shock location to approximately one-half the distance from the shock to the plate; the edge of this bright region was interpreted as the edge of the boundary layer and the bright area as the higher density inviscid region. This presumed boundary-layer edge is compared with that obtained from the pitot pressure and total temperature (T_t)